

Seismic behavior and zoning of the sabkha soils in Jubail industrial city, Saudi Arabia

H. R. Ahmed · N. A. Al Shayea

Received: 9 October 2016 / Accepted: 14 March 2017 / Published online: 2 May 2017
© Springer Science+Business Media Dordrecht 2017

Abstract This study aimed at the micro-level seismic behavior and zoning of the saline sabkha strata in Jubail industrial area in Eastern Saudi Arabia. It encompasses the evaluation of the site-specific seismic response parameters and the liquefaction potential for various possible subsurface conditions under the probable seismic event(s). The approach to achieve the objectives of this study included the following: analysis of geologic, hydrologic, and geotechnical data of the area; performance of field and laboratory dynamic testing; and dynamic modeling and analysis of the subsurface profiles. The results of the simulation have been used to develop liquefaction potential maps and site-specific spectra of the study area, consisting of ten seismic zones under a range of probable peak horizontal ground acceleration (PHA). Results do not show significant probability of liquefaction of the loose soil layers in the study area at the maximum possible design PHA of 0.035 *g*; however, liquefaction is anticipated at higher PHA values. Site-specific spectral response resulted in values of S_s and S_1 spectral accelerations to be different as compared to those suggested by local standards. The resulting

seismic micro-zonation maps and the corresponding parameters are very useful for the stability analysis of the existing and planned structures in the Jubail area.

Keywords Seismic behavior · Seismic zoning · Saline sabkha soils

Abbreviations

ASTM	American Society for Testing and Materials
a_{\max}	Peak horizontal ground surface acceleration
CH	Cross-hole seismic
CRR	Cyclic reduction ratio
D_r	Relative density (%)
FEM	Finite element method
g	Acceleration due to gravity
PHA or PGA	Peak horizontal ground acceleration
PSHA	Probabilistic seismic hazard analysis
PVC	Polyvinyl chloride (pipe material)
S_1	1 s spectral acceleration
SAES	Saudi Aramco Engineering Standard
SBC	Saudi Building Code
SGS	Saudi Geological Survey
S_s	Short-term spectral acceleration (0.2 s)

H. R. Ahmed (✉) · N. A. Al Shayea
Civil Engineering Department, King Fahd University of
Petroleum & Minerals (KFUPM), Dhahran, Saudi Arabia
e-mail: habibrehman@kfupm.com.sa

N. A. Al Shayea
e-mail: nshayea@kfupm.edu.sa

H. R. Ahmed
Riyadh Geotechnique & Foundations (RGF), Al-Khobar, Saudi
Arabia

1 Introduction

Jubail industrial city, located on the west coast of the Arabian Gulf, houses one of the largest and key industrial setups of Saudi Arabia; vicinity map of the Jubail area is

shown in Fig. 1. Since 1977, huge industrial complexes and residential zones have been developed for Jubail industrial city-1, while similar industries are coming for Jubail industrial city-2. Geological depositional processes and subsequent land reclamation processes in the late 1970s resulted in the formation of weak saline sabkha soil layers in the subsurface strata at various depths. Sabkha deposits are characterized by high concentration of salts in the soil and the groundwater. At most of the locations, the salt content of sabkha deposits is as high as sea water (conductivity $\sim 45,000 \mu\text{S}$) and at locations, it has been found to be much higher (conductivity $\sim 208,000 \mu\text{S}$), where groundwater consists of brine (Al-Amoudi 2008). These weak saline sabkha soil layers of varying thicknesses and extent, present across the Jubail area, have always been found to be

problematic even under the static loading of heavy industrial structures. Although these weaker layers have not experienced any major seismic loading in the recent history, they could be susceptible to shear failure, large settlements, and liquefaction under probable moderate seismic event from the nearby seismic sources.

Jubail is about 300 km away from the collision zone of the Arabian and Eurasian plates that stretches across the Zagros Mountains, a prolific source of large-magnitude earthquakes (Al-Amri and Fnais 2011). Historically, earthquakes of magnitude 5+ on the Richter scale are common in this belt, and 6+ magnitude strong quakes occur several times every year, while magnitude 7 events occur every decade. Although the Zagros Mountains are considered as the primary source

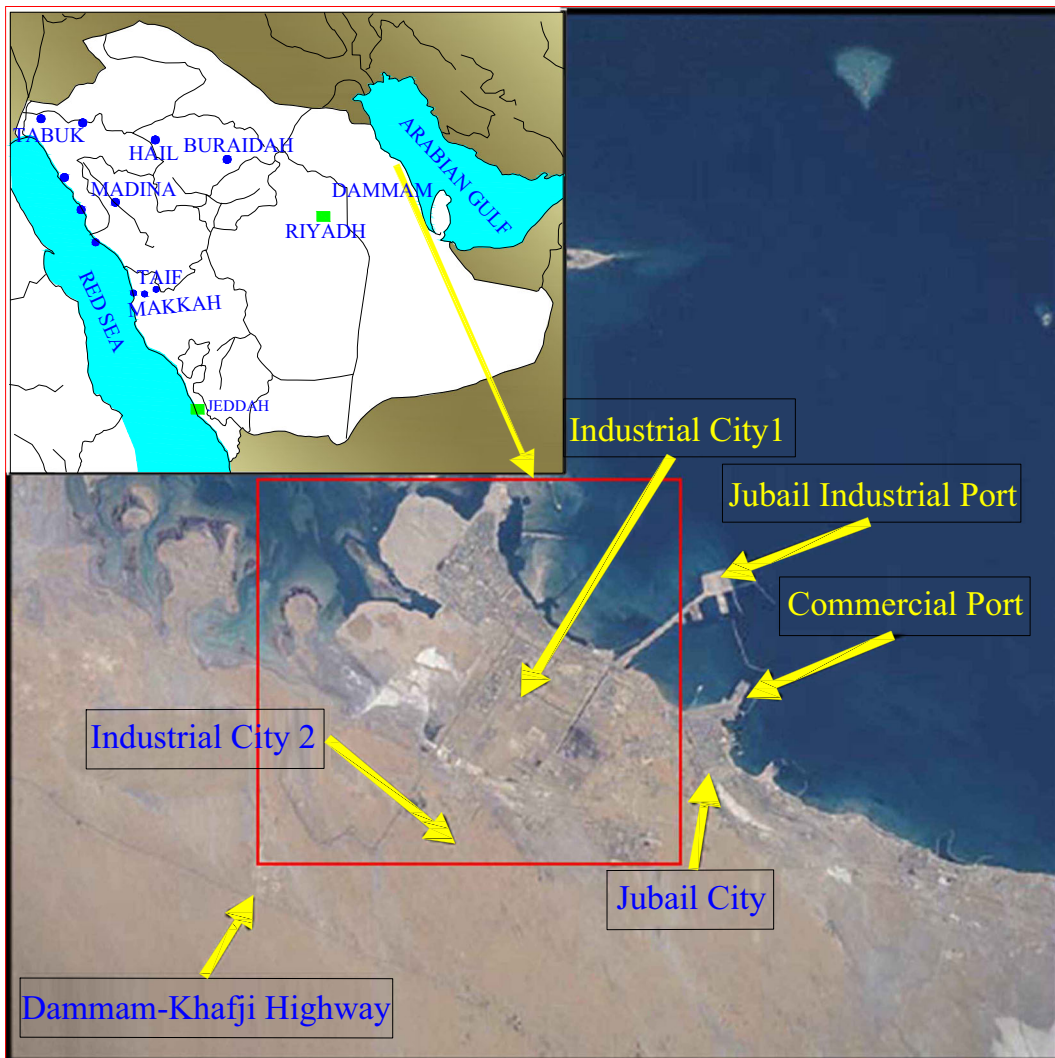


Fig. 1 Vicinity map of Jubail industrial area (from http://en.wikipedia.org/wiki/File:Al_jubail.jpg)

of major earthquakes in the vicinity of the eastern region of Saudi Arabia, an earthquake of magnitude 4.7 occurred on June 2, 1993 in Kuwait. More recent events in Kuwait area include a magnitude 3.9 earthquake on September 18, 1997 and a magnitude 4.2 event on December 30, 1997 (Al-Amri and Fnais 2009). They also reported that a moderately large earthquake the border region of Oman and the United Arab Emirates on January 2002.

In addition to the above, another likely major seismic source is the Makran subduction zone, located at the southern end of the plate boundary, where the Arabian plate around the Gulf of Oman subducts underneath the Eurasian plate. These subduction zones can also result in very large earthquakes; one of the examples is the great Makran earthquake of November 1945 in southern Pakistan with a magnitude of 8.1 (Al-Amri and Fnais 2009). A magnitude 7.8 seismic event also took place in Saravan area of Iran on April 16, 2013, and the tremors were felt all across the eastern region of Saudi Arabia (USGS 2013).

From the above given premise, it is evident that a significant seismic event occurring from any of the above sources may create a geohazard in any city in the eastern part of the Saudi Arabia. Heavily loaded structures coupled with the nature of the subsurface strata in Jubail area may lead to the undesirable consequences on the existing structures under any probable seismic event. Although several local corporations have furnished seismic design recommendations and standards for various locations in Saudi Arabia e.g., SAES-A-112 (2013), many of them are very general and provisional in nature. Moreover, these recommendations are based on the macroseismic zoning concept, and do not consider the site-specific seismic response for the variations in subsurface strata conditions within a city and/or a region. As site-specific response plays a crucial role in the stability analysis of structures, it has become imperative to perform micro-level seismic zoning for major cities along the east coast of Saudi Arabia. Site-specific seismic studies of the area should be conducted to assess the site-specific response and possible adverse effects of the probable seismic activity. Moreover, no study was found on the dynamic characterization and seismic evaluation of saline sabkha soils. Therefore, this study aimed at development of micro-level seismic zoning of the Jubail industrial area, encompassing assessment of the site-specific seismic response parameters and the liquefaction potential for various possible subsurface conditions, under probable seismic event(s).

2 Methodology

In order to achieve the stated objectives, the approach of this study consisted of the following: analysis of geologic, hydrologic, and geotechnical data of the area, and data relevant to the seismic micro-zonation; conducting field and laboratory testing on sand and sabkha samples; assessment and formulation of dynamic model profiles; and performing dynamic modeling and analysis of the subsurface profiles using finite element method (FEM)-based computer software. These tasks are detailed in the following sections.

2.1 The study area

This section discusses the geologic, hydrologic, and geotectonic settings of the study area. The Arabian Peninsula is divided geologically into two structural parts, namely the Arabian Shield located to the west, and the Arabian Shelf located towards the east (Al-Sayari and Zotl 1978). Jubail city is part of the Arabian Shelf, where the rocks and soils in the area are a result of marine and continental sedimentation processes that prevailed in the past, which resulted in the presence of unconsolidated materials of Tertiary age and sediments of Quaternary age. The surface geology of the Jubail area generally consists of young, poorly consolidated but occasionally cemented deposits of Quaternary age composed of mobile or relatively stable vegetated dunes, coastal deposits, and sabkha (James and Little 1994).

These near-surface deposits are underlain by the older (Neogene) Hadrukh formation present as the bedrock in the area, and occasional small outcrops are found at the surface. Sand dunes are present as small hills at the margins of the sabkha deposits and mostly composed of fine to medium sand with a little silt content. At places, these sand dunes cover the Hadrukh formation to a few meters below the dune's surface. A layer of limestone or cemented sand, known locally as "caprock," occurs at places on top of the coastal deposits. Sabkha soils, covering about 40% of the industrial complex, vary from very soft gypsiferous muds to loose and fine to medium sands with or without lenses of gypsum, halite, and other salts' crystals. Underlying Hadrukh formation consists of alternations of sandstone, limestone, marl, and stiff to very stiff clays and silts. The layers of sandstone may be found as weakly or strongly cemented. James and Little (1994) came up with a

detailed map of the Jubail industrial city marking the presence and boundaries of the sabkha regions, while a similar map has also been prepared by Saudi Geological Survey (SGS 2009).

Water aquifers existing at the area could be divided into shallow (<50 m) and deep. Shallow aquifer occurring in Quaternary deposits and Hadruk formation is called Neogene aquifer. Most of the recharge in the shallow aquifer in the Jubail industrial area is from the seawater, while some areas towards the western side receive recharge from the sporadic rains. The local water table, in Jubail area, follows the tidal variations of the sea water level. It also fluctuates during the summer by one half to 1 m, while it rises during winter months, the water table rises and combines with additional rainfall, to cover much of the ground surface of low lands.

2.2 Tectonic and seismic design parameters

The Arabian Peninsula makes up the majority of the Arabian plate. The plate is moving towards northeast direction (Al-Haddad et al. 1994). This movement is accompanied by collision with and subducting beneath the Eurasian plate, which are manifested by the seismicity of the region. Figure 2 (Fnais 2011) identifies the seismotectonic zones that could impact the eastern region in general and Jubail, in particular with the corresponding maximum intensity earthquake.

Peak horizontal ground acceleration (PGA or PHA) and response spectra represent the main parameters required for seismic hazard assessment and for design of earthquake-resistant structures. For site-specific seismic study, the input parameters required are the design earthquake at the bedrock and the geophysical/geotechnical

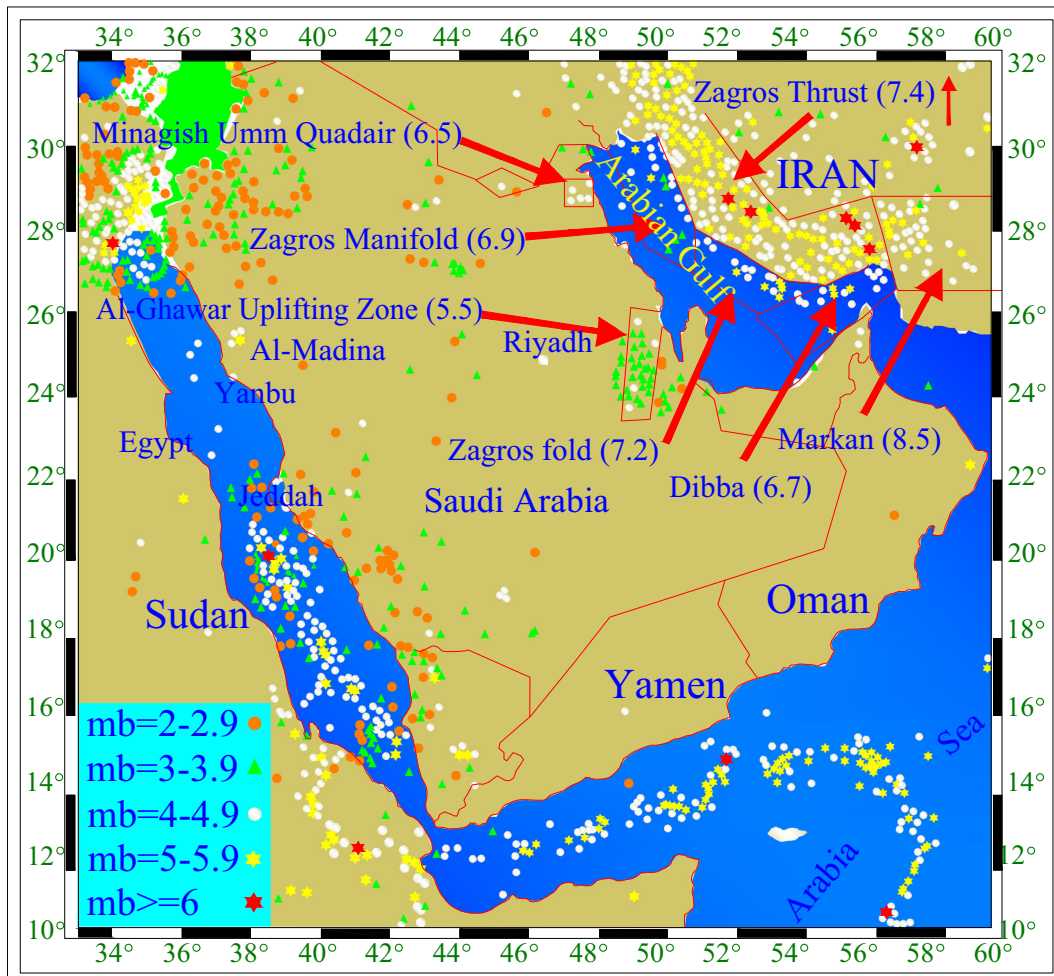


Fig. 2 Seismic source zones affecting the eastern province of Saudi Arabia (after Fnais 2011)

design parameters assigned to the soil column overlying the bedrock. A design earthquake is defined as the earthquake with a 10% probability of exceedance in 50 years (Kramer 1996). Due to the absence of strong ground motion records for the considered area, the previous hazard studies in Saudi Arabia (Al-Amri et al. 2008; Peiris et al. 2006; Sadek 2004; Abdalla and Al-Homoud 2004a, 2004b; Al-Haddad et al. 1994) borrowed attenuation models for other areas to calculate the ground motion parameters. However, Fnais (2011) adopted an approach for estimating the ground motion attenuation relation for the area based on the seismological model of Boore (2003) and attenuation model by Joyner and Boore (1981) to study the seismic activity from five possible sources of seismic activity for area (Fig. 2). Out of these five possible sources, Kuwait seismic zone could be considered the nearest source to the Jubail area. Hence, the study area is vulnerable to seismic hazard due to the presence of a thick section of the sediments.

PHA values for the eastern province of Saudi Arabia were simulated for moment magnitudes (M) ranging from 4.0 to 6.5, at 0.5 increments. The upper bound of magnitude range was selected to be 6.5 representing the maximum magnitude that can be produced from Kuwait seismogenic source. The distance from the fault was divided into 18 increments from 1 to 300 km, representing the shortest distance between the projection of the rupture and the study area. Jubail area could be the most vulnerable to an event originating in Kuwait, approximately 230 km to the north. The expected peak bedrock ground acceleration is 0.025 g (24.5 cm/s^2) based on attenuation relationship developed by Fnais (2011). The local geology and topography effects control the distribution of damages due to strong earthquakes. The amplification of earthquake ground motion by local site conditions is required to be estimated in areas characterized by soft sediments.

For the dynamic simulation purposes, a maximum possible design input earthquake has been selected based on the knowledge of the probable seismic activity in the area. The selected input earthquake was acquired mainly from seismic design codes by Saudi Aramco (SAES-A-112 2013), Royal Commission (RC Engineering Manual 2006), and Saudi Building Code SBC-303 (2007). The design recommendations by Saudi Aramco standard SAES-A-112 (2013) are provided as macroseismic zoning of KSA and the corresponding seismic design parameters. Pascucci et al. (2008), based on their detailed probabilistic seismic hazard

analysis (PSHA), proposed seismic response parameters for the various cities of the Arabian Gulf region.

All the above-referenced standards and studies lead to the conclusion that maximum PHA of 0.035 g, as suggested by Saudi Aramco SAES-A-112 (2013), was adopted for the dynamic modeling purpose. Due to lack of any past earthquake accelerogram of the area, the seismic simulation adopted a synthetic earthquake of 10 s duration and PHA of 0.035 g from the earthquake records database of Saudi Geological Survey (SGS) and is shown in Fig. 3. This was considered as the base intensity earthquake for the analysis purposes. This intensity was increased, incrementally till liquefaction occurred.

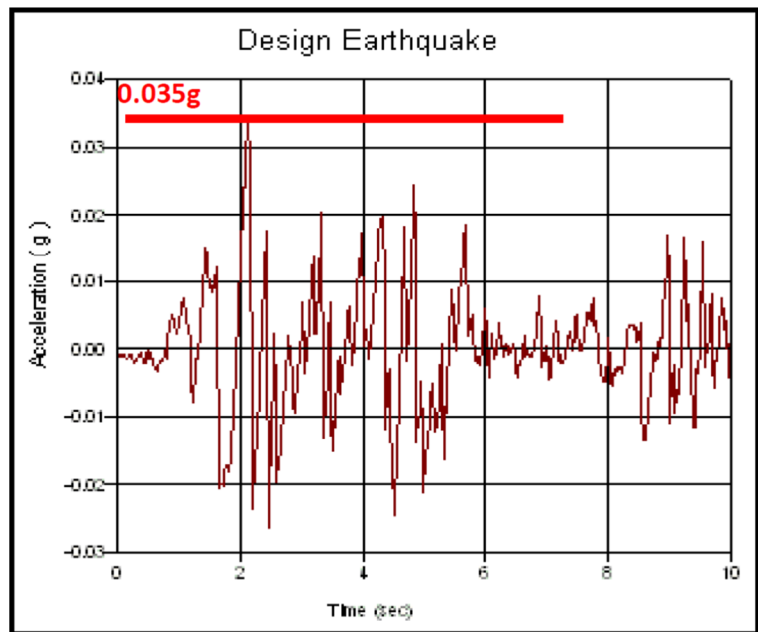
2.3 Laboratory tests

Samples from several soil layers encountered in Jubail area were subjected to various classification and characterization tests. The classification tests comprised grain size distribution (ASTM D422 2007) and Atterberg limits (ASTM D4318 2010). The strength parameters of various strata across the area were ascertained mainly through direct shear tests (ASTM D3080 2011), and consolidated undrained (CU) triaxial compression tests (ASTM D4767 2011). The drained strength parameters were assessed from the undrained strength and the recorded pore pressures. The range of test results representing the typical soil layers present in the study area is summarized in Fig. 7.

2.4 Field and laboratory dynamic data acquisition

Dynamic design parameters of the various soil layers of the subsurface strata are expressed as compression wave velocity (V_p) and shear wave velocity (V_s), shear modulus, damping ratio, and their attenuation with shear strain. In this study, V_p and V_s were initially assessed from the available geotechnical/geophysical investigation reports, and were further acquired from the additional cross-hole field seismic tests. Cross-hole seismic tests (ASTM D4428 2007) were carried out at seven selected locations in the various defined subsurface strata zones of the study area and were used for the evaluation of dynamic properties of the subsurface strata, i.e., dynamic Young modulus and dynamic shear modulus. Standard penetration tests (SPTs) were also carried out (as per ASTM D1586 2011) in all the typical soil layers in each of the boreholes of the cross-hole tests to obtain standard N_{60} values. Disturbed sand and

Fig. 3 Proposed earthquake accelerogram for the Jubail industrial area (adapted from QUAKE/W software database)



sabkha samples, acquired during the borehole drilling, were subjected to laboratory cyclic triaxial and resonant column tests. This is to obtain shear modulus and damping characteristics and to assess liquefaction potential.

2.4.1 Cross-hole seismic tests

Cross-hole seismic tests were conducted at the specified depth horizons as per ASTM D4428 (2007) using the Olson CS Equipment. In each test, three boreholes, spaced 3.0 m apart center to center, were drilled in a straight line to a depth of 30.0 m. After drilling, PVC pipes were lowered in the holes, and the annular space was grouted to ensure a perfect contact between the strata and the PVC pipe. After the grout had set, a borehole inclination survey was carried out to precisely determine the distance between the boreholes at several depth intervals. The seismic waves were generated in one of the boreholes (the shot hole), and its horizontal travel time was recorded in the other two boreholes (the receiver holes). The seismic waves were generated using the specially designed shear and normal waves producing hammer. The readings were recorded at every 1.0 m interval down to the maximum depth of 30.0 m. The results of the field cross-hole seismic tests for two typical subsurface profiles are shown in Fig. 4.

2.4.2 Laboratory cyclic triaxial tests

Laboratory cyclic triaxial tests (ASTM D5311 2011) were carried out on samples collected from the field to determine the full spectrum of the dynamic parameters under various probable subsurface scenarios as per the testing schedule provided in Table 1.

The collected samples were subjected to grain size analysis and density tests. Maximum and minimum density values were used to obtain the required relative density (D_r) levels for the cyclic triaxial tests. To simulate the various density levels of the subsurface sand strata ranging from loose sandy sabkha to very dense sand layers of the Hadruk formation, D_r values of 40, 60, 75, and 85% were selected. Specimens were prepared to achieve these densities. Specimens of 50 mm diameter and 100 mm height were prepared in five layers using the compaction criteria guidelines of Amir et al. (2012) to achieve a uniform relative density in the specimen.

In this study, the specimen preparation technique was selected to simulate the natural conditions of the study area. The loose sand deposits in the study area are windblown in nature that got compacted, later on, due to overburden pressure. In order to simulate these processes, specimen preparation was made using a combination of pluviation and tamping based on the works of Mitchell et al. (1976), Mulilis et al. (1977), Been and Jefferies (1985), Tatsukao et al. (1986), Canou (1989),

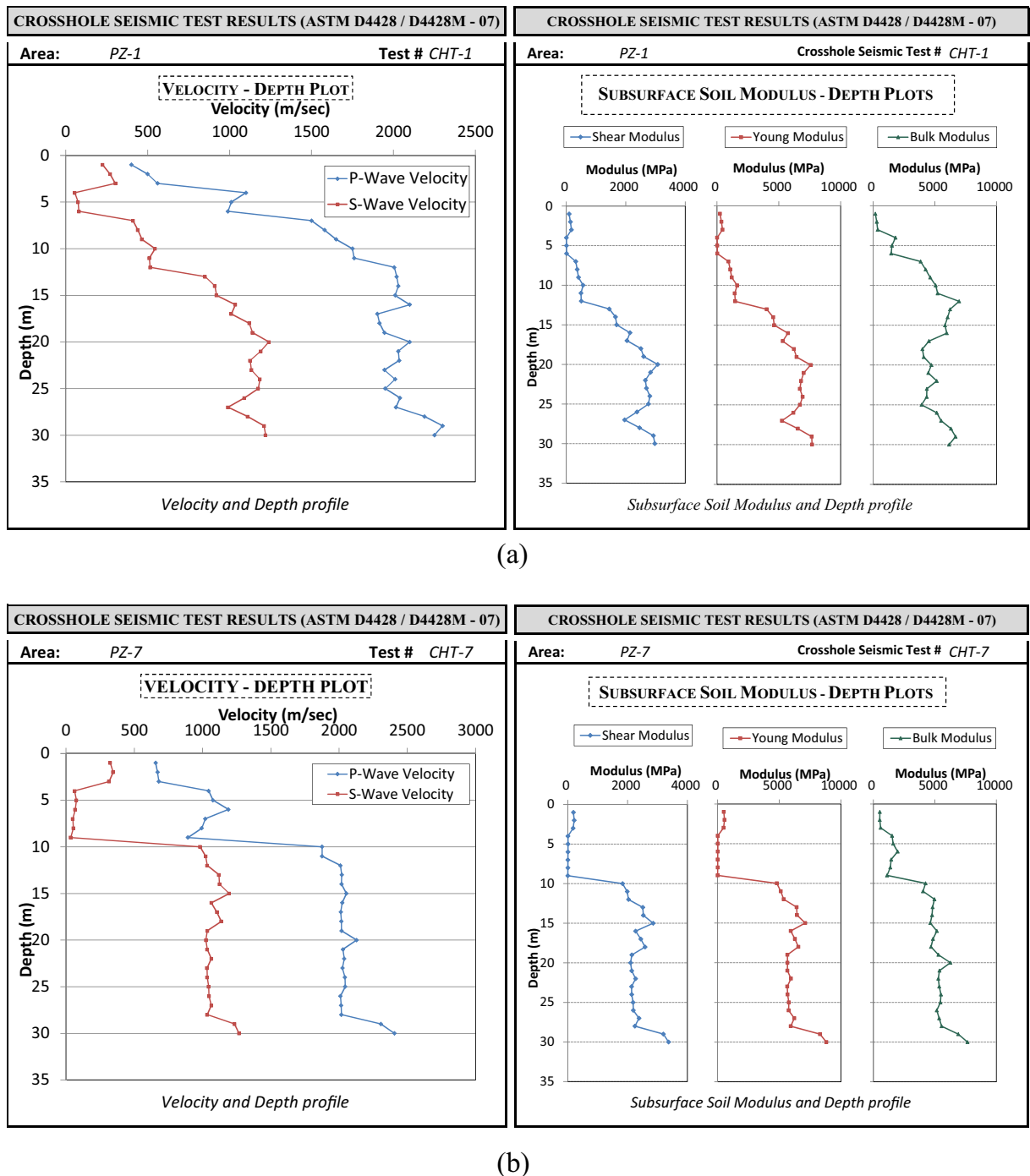


Fig. 4 Cross-hole seismic test results showing variation of V_p , V_s , and modulli for **a** zone 1 and **b** zone 7. Sharp increase in V_p at about 3.0–4.0 m depth indicates the presence of water table

Zlatovic and Ishihara (1997), Vaid et al. (1999), Juneja and Raghunandan (2010), and Benahmed et al. (2015) to replicate the depositional and consolidation/compression processes during their formation. Each

sand layer was pluviated in the mold and then compacted by tamping to the desired density. After compaction, the specimens were saturated with saline water obtained from the ground water of the study area.

Table 1 Laboratory testing program for cyclic triaxial tests on sand samples

Relative density (%)	Confining pressure (kPa)	Stress ratios	Frequency (Hz)
40	100	0.7, 0.5, 0.3, 0.1	0.1, 1.0
60	150	0.8, 0.6, 0.4, 0.2	0.1, 1.0
75	200	0.8, 0.6, 0.4, 0.2	0.1, 1.0
85	300	0.8, 0.6, 0.4, 0.2	0.1, 1.0

In this way, the prepared specimens had the structure (both the fabric and the interparticle forces) that closely resembled that of the soil in the field. The saturation step was followed by applying the confining pressure. At the end of the application of confining process, drain valve was closed, and the test specimen was subjected to the deviator cyclic stress of the specified frequency.

For each D_r value, the cyclic loading tests were conducted for the specified confining effective pressure and the variation of stress ratios and the cyclic frequencies. Stress ratio is defined as the sum of the compression and extension cyclic stress (in excess of the effective confining pressure) divided by the effective confining stress. Cyclic triaxial tests were conducted for each of the specified parameter combinations as per Table 1. To study the liquefaction potential, the number of cycles required to reach liquefaction was obtained for each relative density, stress ratio, frequency, and confining pressure. Typical results are shown in Fig. 5.

For the determination of dynamic Young's modulus of elasticity, specimens were prepared in the same manner as described earlier. The compacted specimens, after saturation and consolidation, were subjected to an

incremental stress ratio of 0.025. Each loading step was continued for a total of 10 cycles. The value of the load, deformation, and hysteresis loop (stress-strain curve) of the last cycle of each step was used to calculate dynamic Young's modulus and damping ratio.

2.4.3 Resonant column tests

Resonant column test was carried out as per ASTM D4015 (2015). The test apparatus consisted of a steel cell, magnetic coil assembly to produce a sinusoidal torsional force to the top of the specimen, charge amplifier, oscilloscope (to display sinusoidal signal and x - y plot to set up resonance), voltmeter for measuring the applied sinusoidal signal in terms of g/V , and function generating device to induce a sinusoidal signal with variable frequency. The procedure for the specimen preparation and saturation was the same as in cyclic triaxial test; however, the prescribed consolidation effective stress was reached in four equal steps. At each step, sufficient time was given for consolidation till complete dissipation of pore pressure had occurred. The resonant frequency and shear modulus were determined at each consolidation stage by inducing a very low-level shear strain so that no pore pressure is developed while drainage is kept closed.

For determining resonant frequency, a sinusoidal torsional signal was applied to the top end of the specimen, and the frequency of the applied torsional force was adjusted so that it became equal to the first mode of natural frequency of the specimen. The process was repeated for each consolidation stage to reach the final consolidation; then, the drainage was closed after complete dissipation of

Fig. 5 Typical cyclic triaxial test results for the sand specimen at $D_r = 75\%$, stress ratio = 0.4, frequency = 1 Hz, and confining stress = 100 kPa

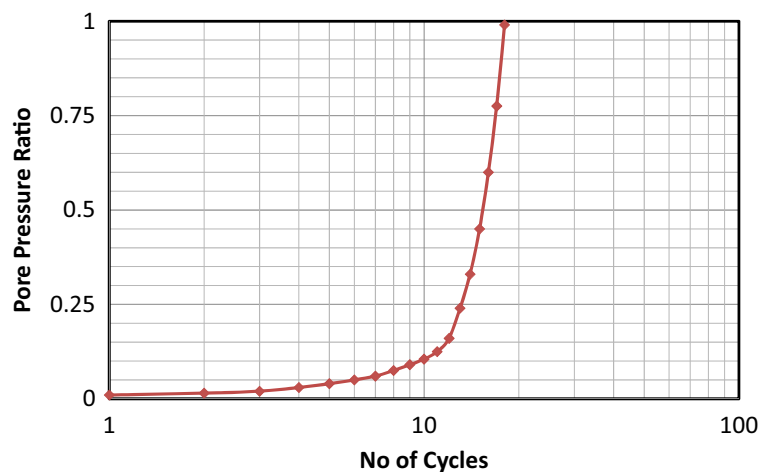
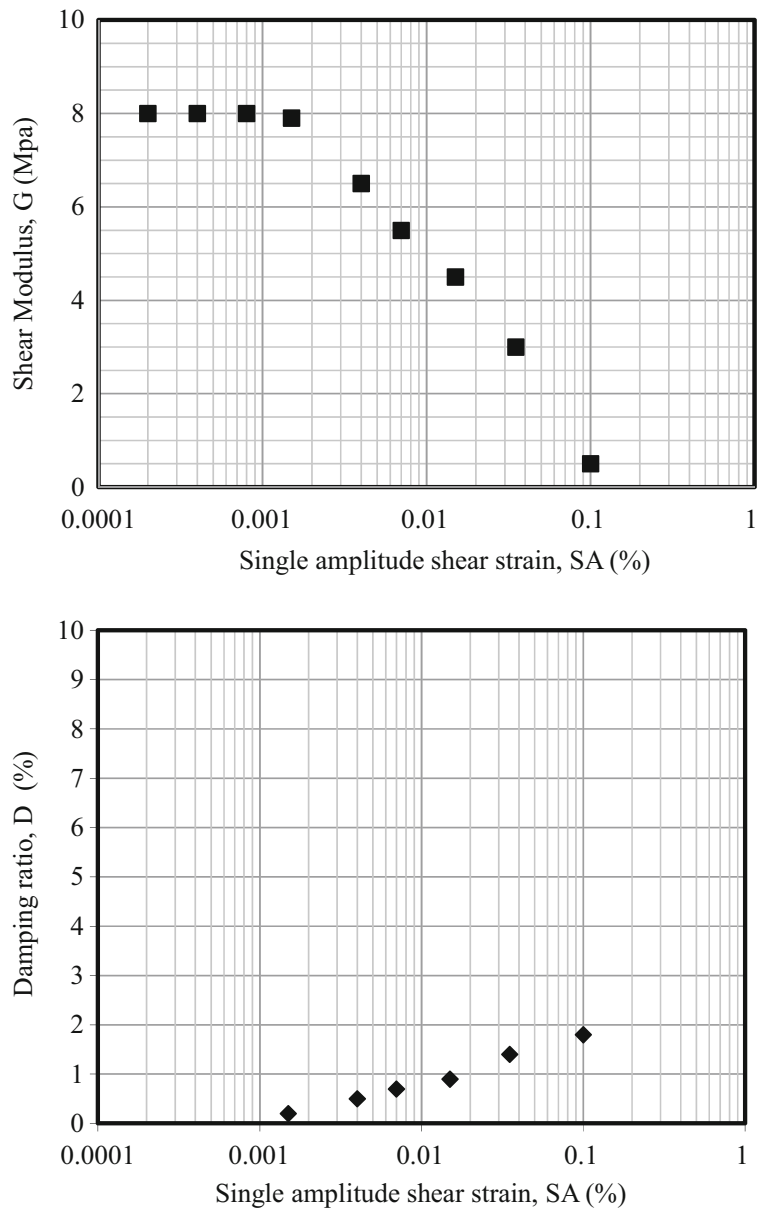


Fig. 6 Typical resonant column test results showing variation of shear modulus and damping ratio against single amplitude shear strain for the sand specimen at $D_r = 75\%$



pore pressure at the end of final consolidation step. The specimen was subjected to sinusoidal torsional force starting from very low shear strain level, to determine the resonant frequency at each shear strain level, and allow for dissipation of any pore pressure before proceeding to higher signal levels. At the ultimate stage, the damping was also recorded at comparatively higher shear strains. The test was terminated at the stage when the excess pore pressure developed due to high strain level, which resulted in higher shear strains. It was observed that with an increase in density and effective confining pressure,

resonant frequency and shear increased, while damping decreased. Typical results are shown in Fig. 6.

2.5 Zoning and subsurface strata profiling of the study area

From the geology of the study area, it was evident that the unconsolidated Quaternary deposits prevail as the near surface strata. There are sand, sabkha, and hard Hadruk formation clay layers present at various depths of the study area. These deposits will amplify ground motion in case of

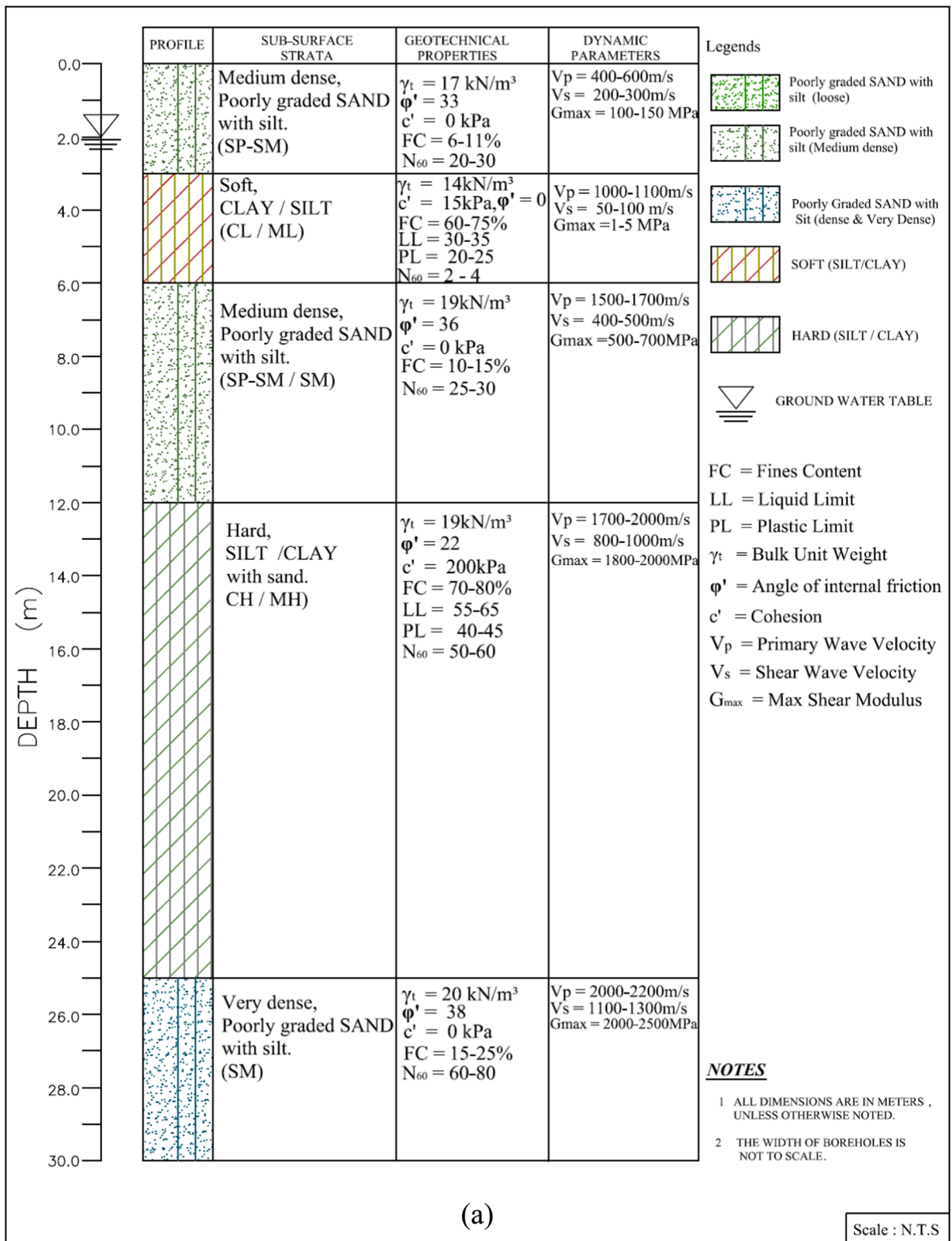


Fig. 7 Subsurface design sections showing various soil layers with corresponding geotechnical static and dynamic design parameters for **a** zone 1 (PZ-1), **b** zone 2 (PZ-2), and **c** zone 7 (PZ-7)

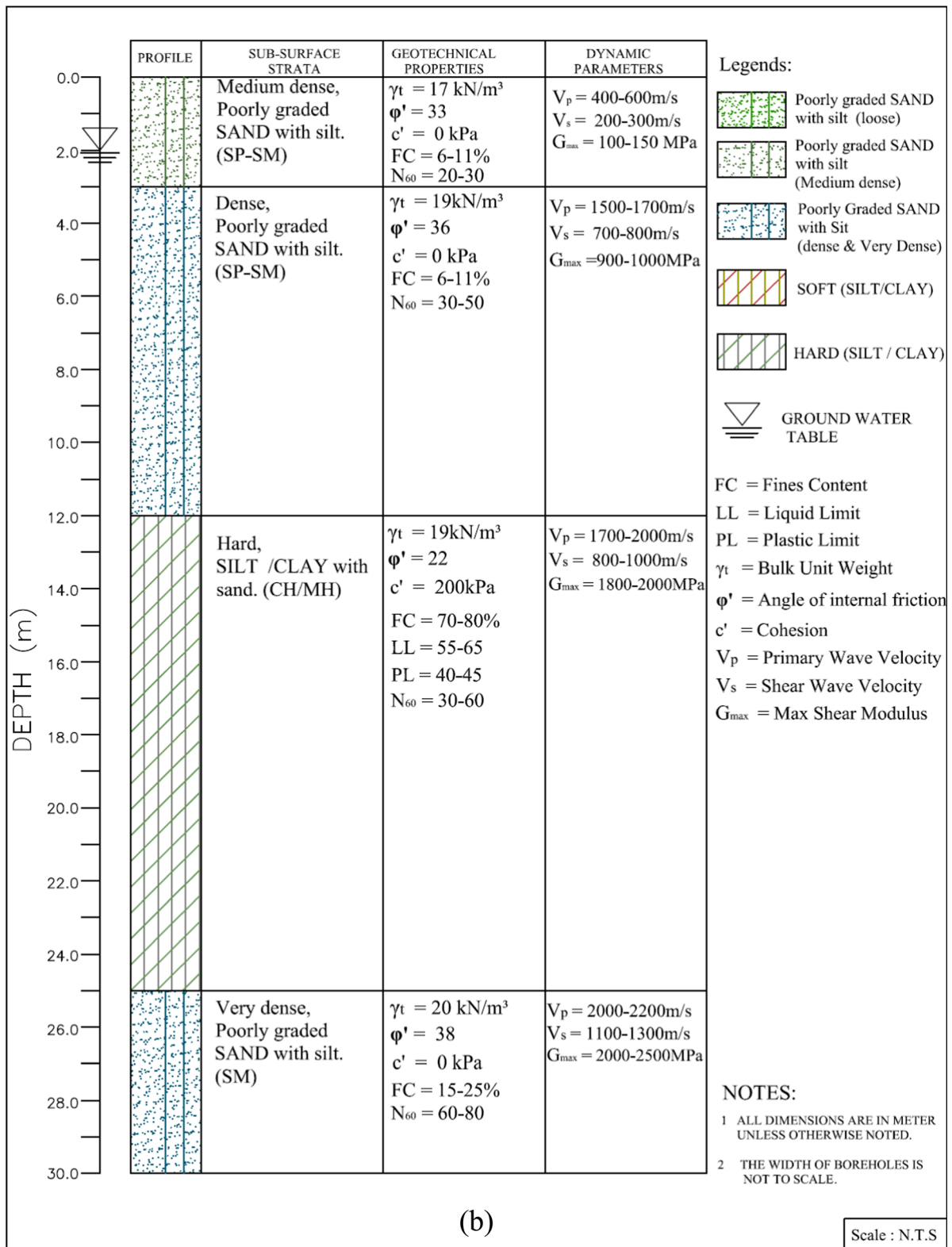


Fig. 7 (continued)

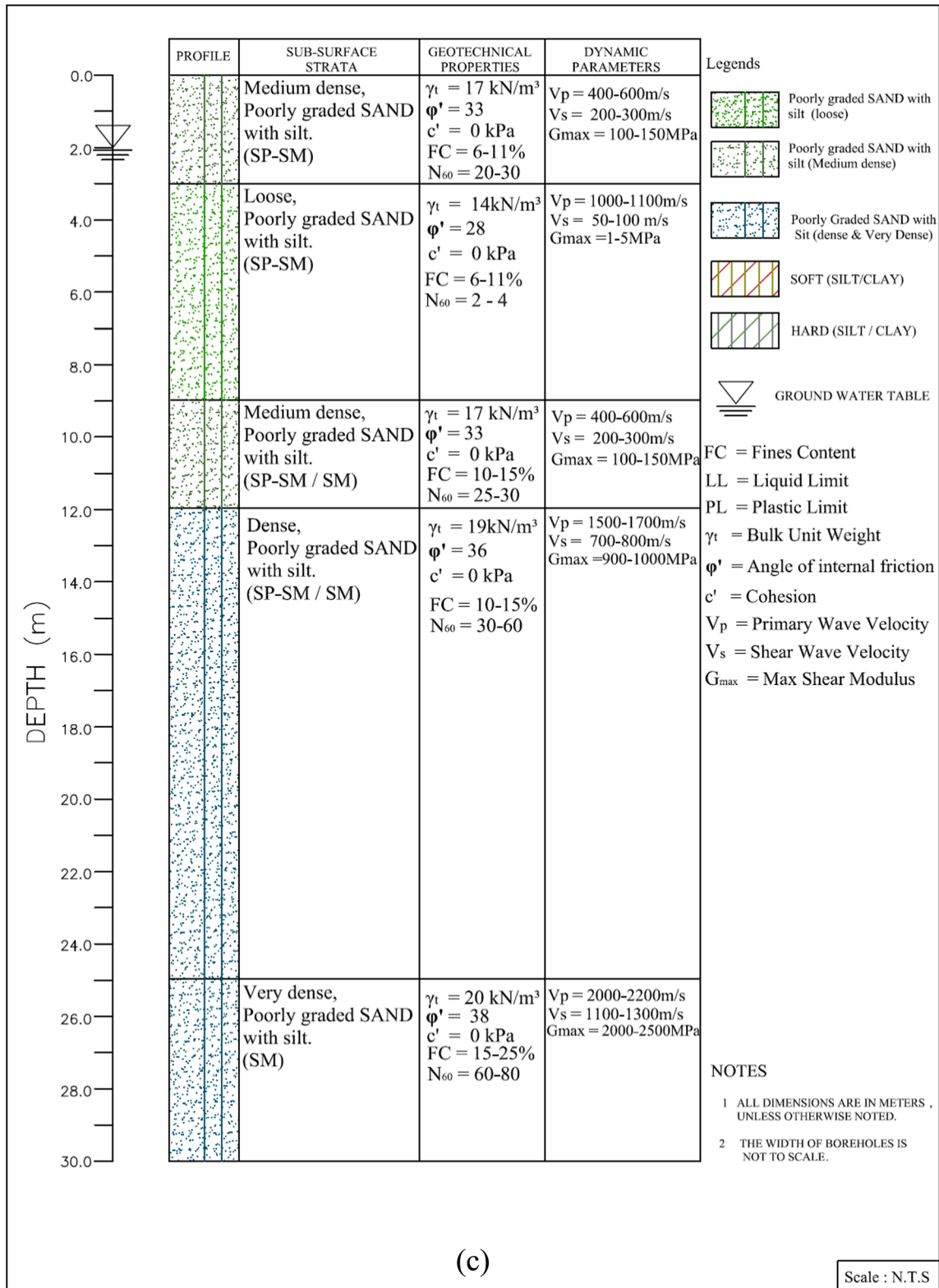


Fig. 7 (continued)

seismic event. The sabkha consists of sandy or clayey soils and seabed materials, overlain by reclaimed sand layers of about 2 to 6 m thick, at most of the locations. The underlying sands over the hard clay of Hadruk formation are present in medium to very dense conditions. Due to variations in the depositional environment, variations are observed in the type, thickness, and depth of various subsurface layers found within the depth of 30.0 m. Based on these variations, the area was divided into ten different seismic zones. As an example, typical subsurface profiles for zone 1 and zone 7 are shown in Fig. 7.

2.6 Dynamic modeling and simulations

Dynamic modeling and analysis were performed to acquire the final design profiles for each zone of the study area using QUAKE/W software (version 5.16) by

GEO-SLOPE International (www.geo-slope.com 2003). Several variations of models were prepared in the software as per the general zoning. Various levels of earthquake shaking were imposed on these models, starting from 0.035 g to the values causing liquefaction.

For all the typical subsurface layers, results were plotted for the variations of design parameters (such as damping ratio, shear modulus, pore pressure and shear stress ratio) versus the corresponding shear strain or the number of cycles. Some typical plots of such variations are shown in Fig. 8.

Modeling requires the formulation of an in situ stress model as a first step. This initial stress model was created using the static design parameters of modulus of elasticity and Poisson’s ratio. The water table was also defined in this model at the corresponding elevation. The typical model for zone 1 is shown in Fig. 9.

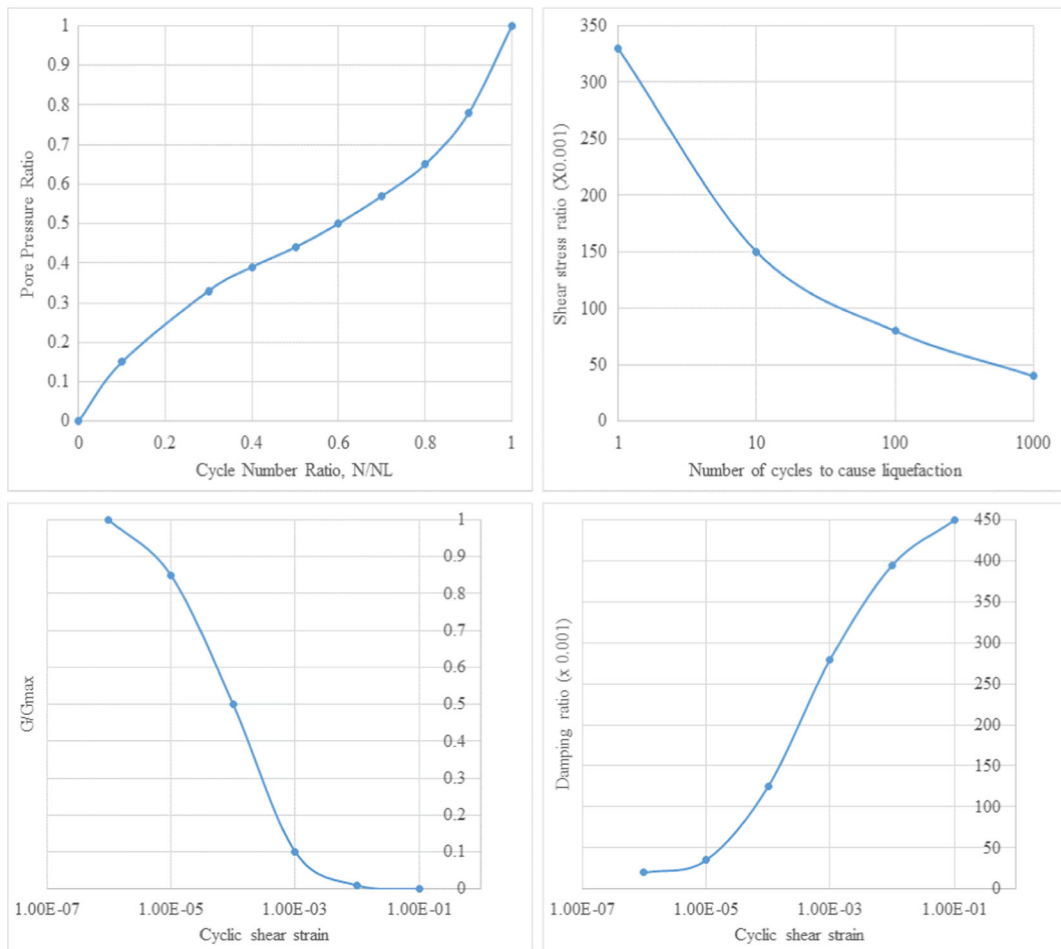


Fig. 8 Variation of pore pressure functions, shear stress ratio, damping ratio, and shear modulus used for various layers in QUAKE/W models

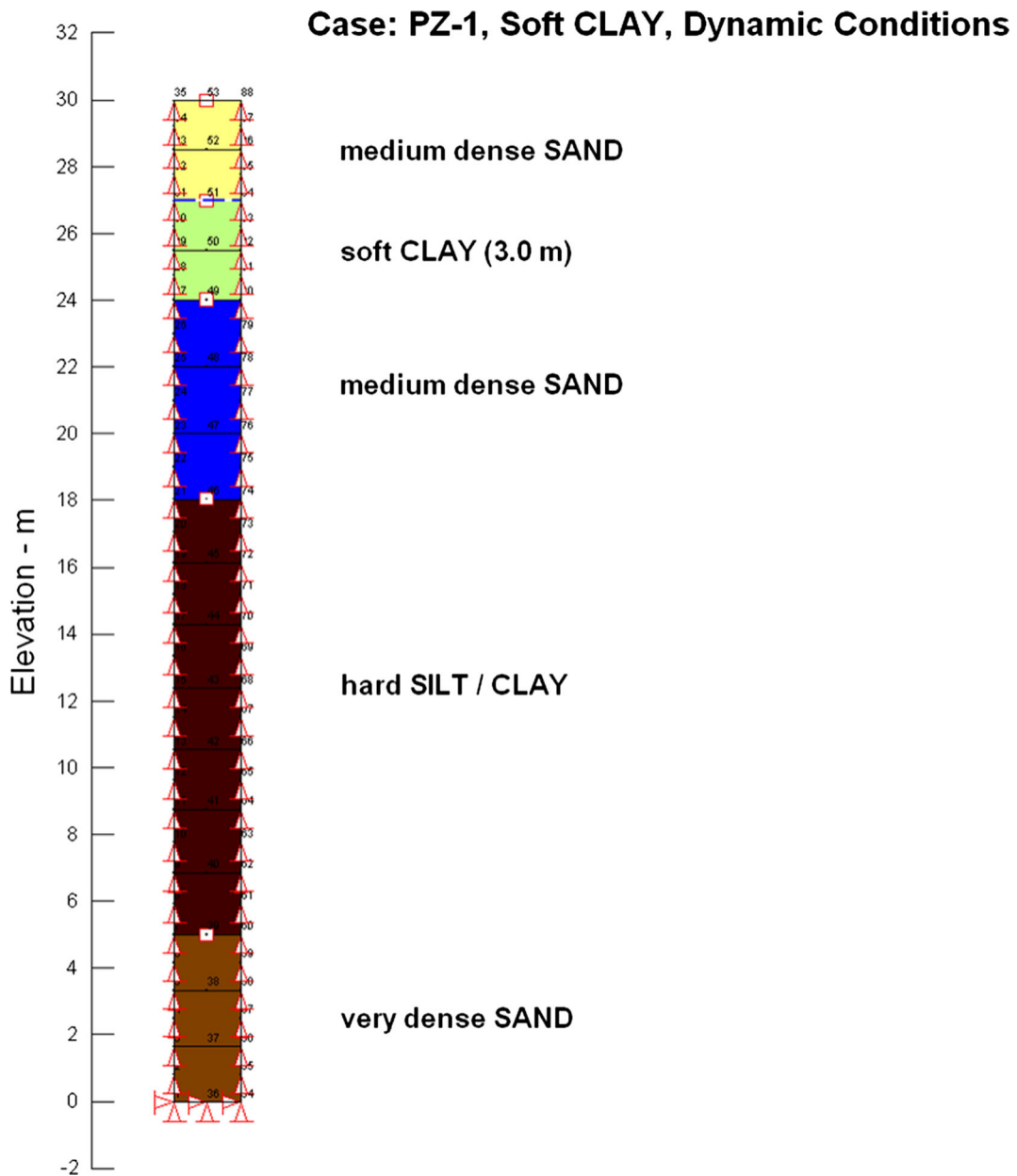
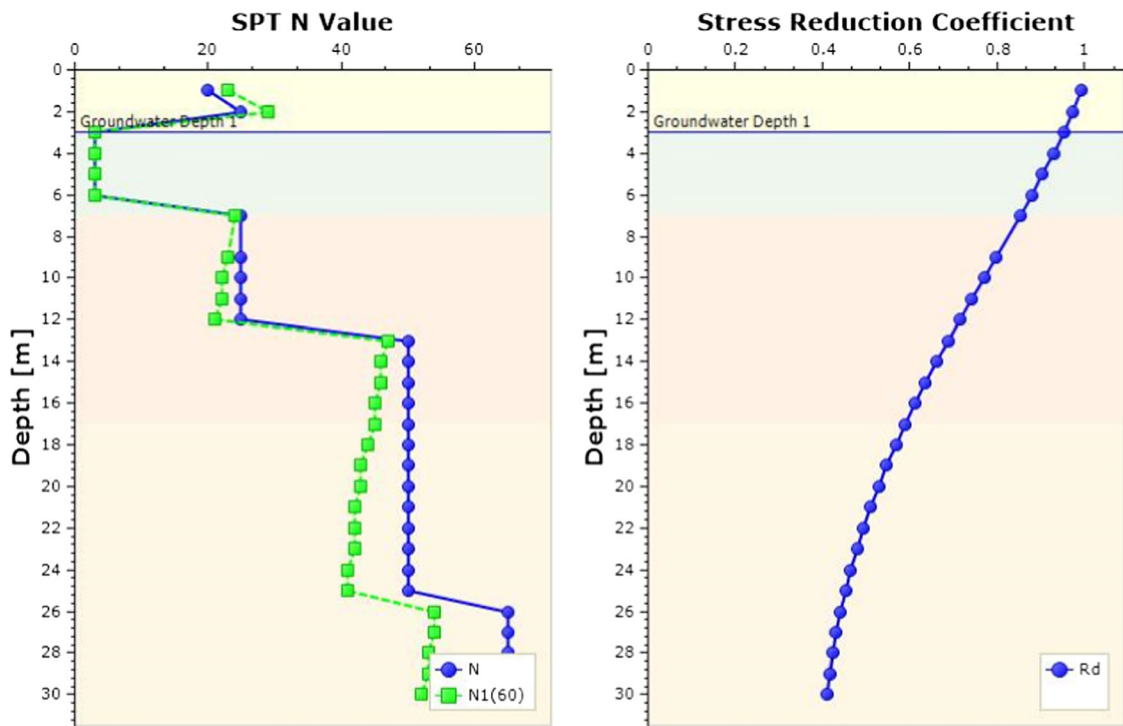


Fig. 9 Model PZ-1 in QUAKE/W software representing the subsurface layers and their seismic and geotechnical properties for zone PZ-1

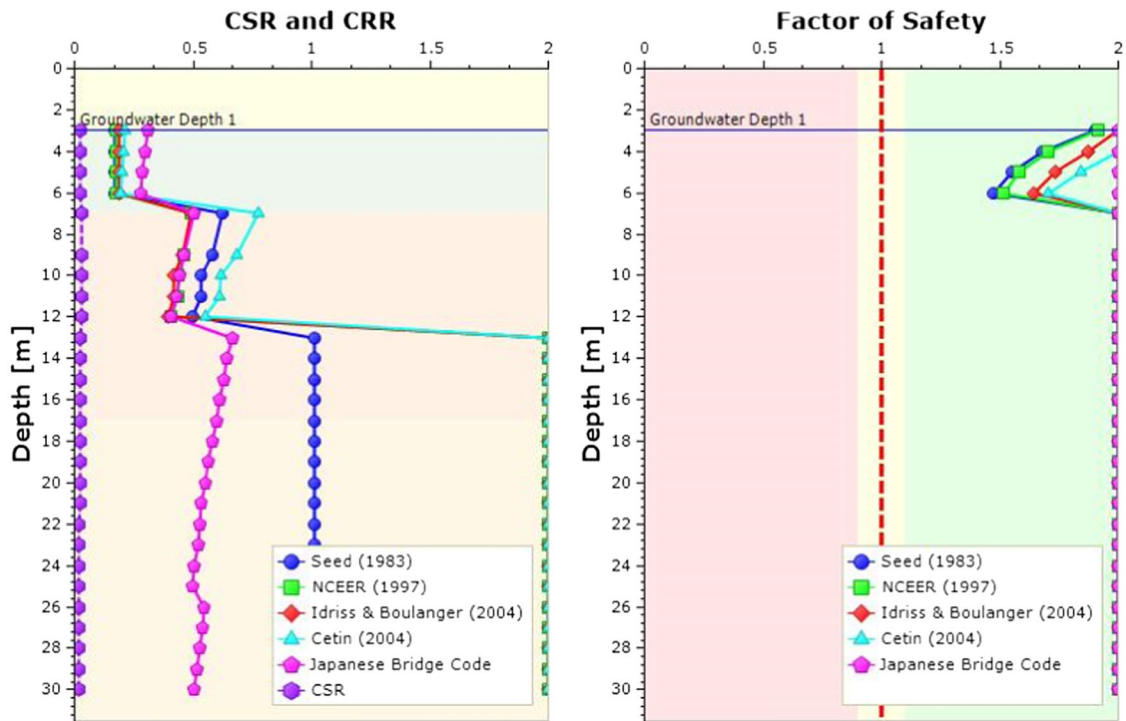
The initial stress model acts as a source of in situ stresses and pore pressure for the dynamic model. The dynamic model was created using the dynamic parameters and their variations with shear strain and number of cycles. For more precision, each force increment was numerically divided into 500 steps.

Liquefaction was assessed in the software by the initiation of the yield zones in the liquefaction-prone

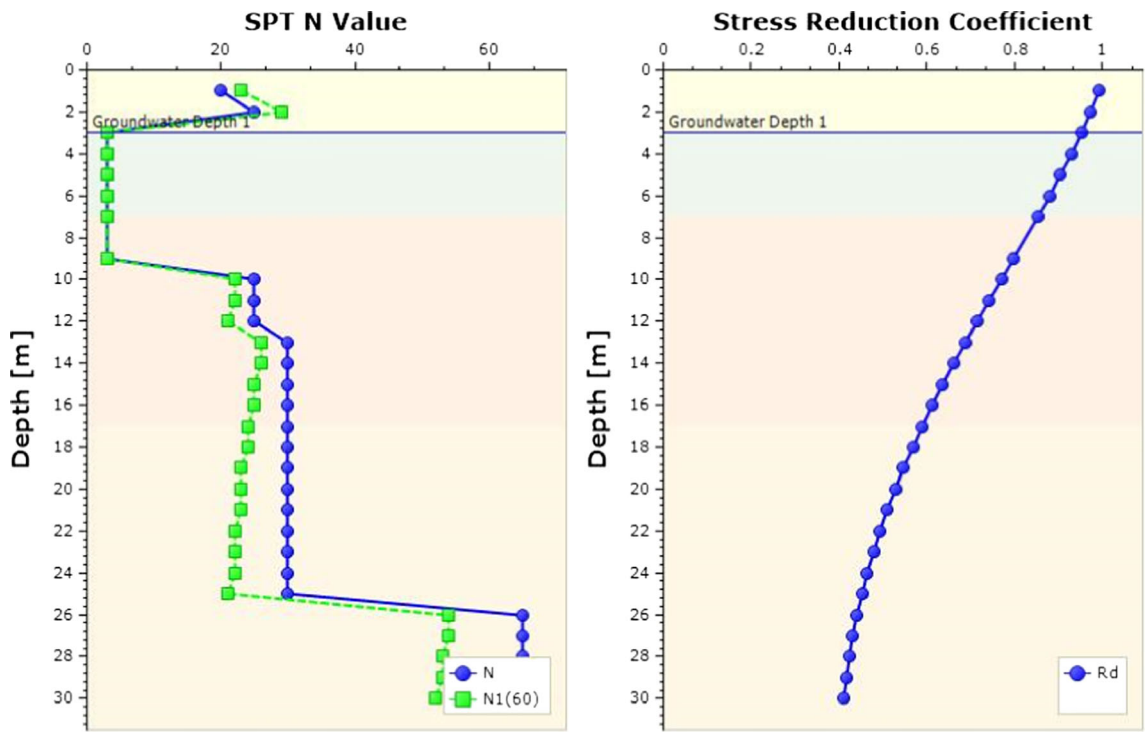
Fig. 10 Results of liquefaction potential determination for zone 1 (PZ-1) and zone 7 (PZ-7) using Settle3D software. **a** SPT and stress reduction coefficient variation with depth for zone 1, PGA = 0.035 g. **b** CSR, CRR, and liquefaction potential variation with depth for zone 1, PGA = 0.035 g. **c** SPT and stress reduction coefficient variation with depth for zone 7, PGA = 0.035 g. **d** CSR, CRR, and liquefaction potential variation with depth for zone 7, PGA = 0.035 g. **e** CSR, CRR, and liquefaction potential variation with depth for zone 7, PGA = 0.06 g



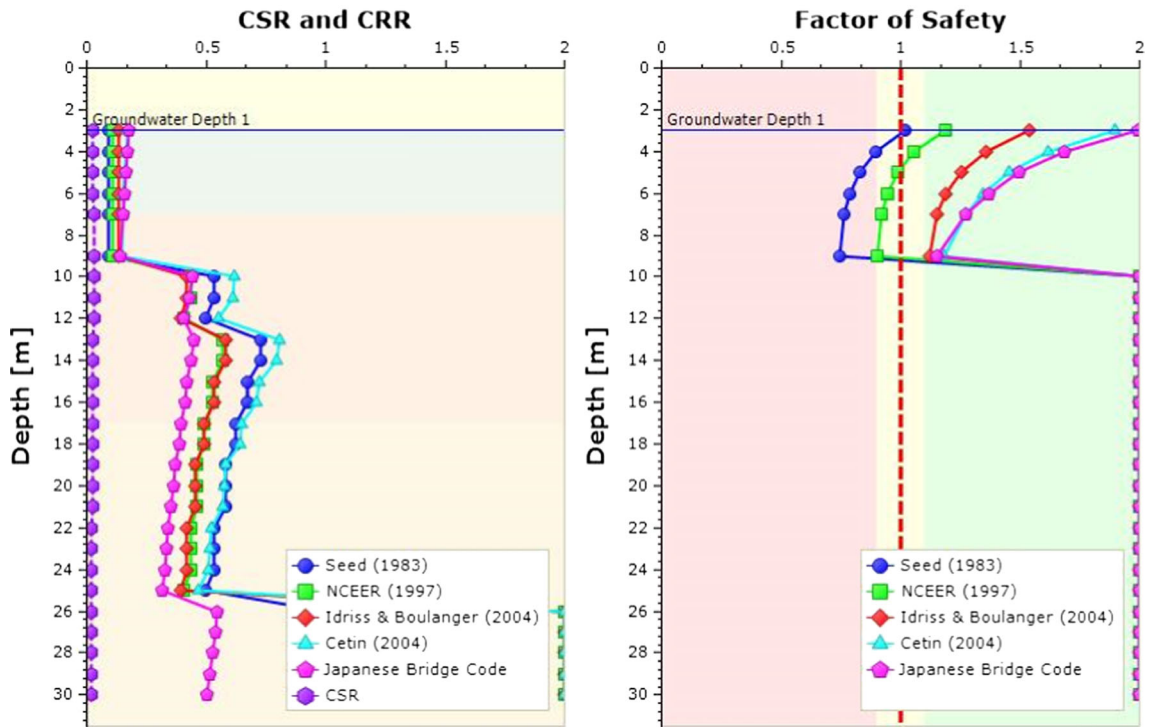
(a) SPT and stress reduction coefficient variation with depth for Zone 1, PGA=0.035g



(b) CSR, CRR, and Liquefaction potential variation with depth for Zone 1, PGA=0.035g

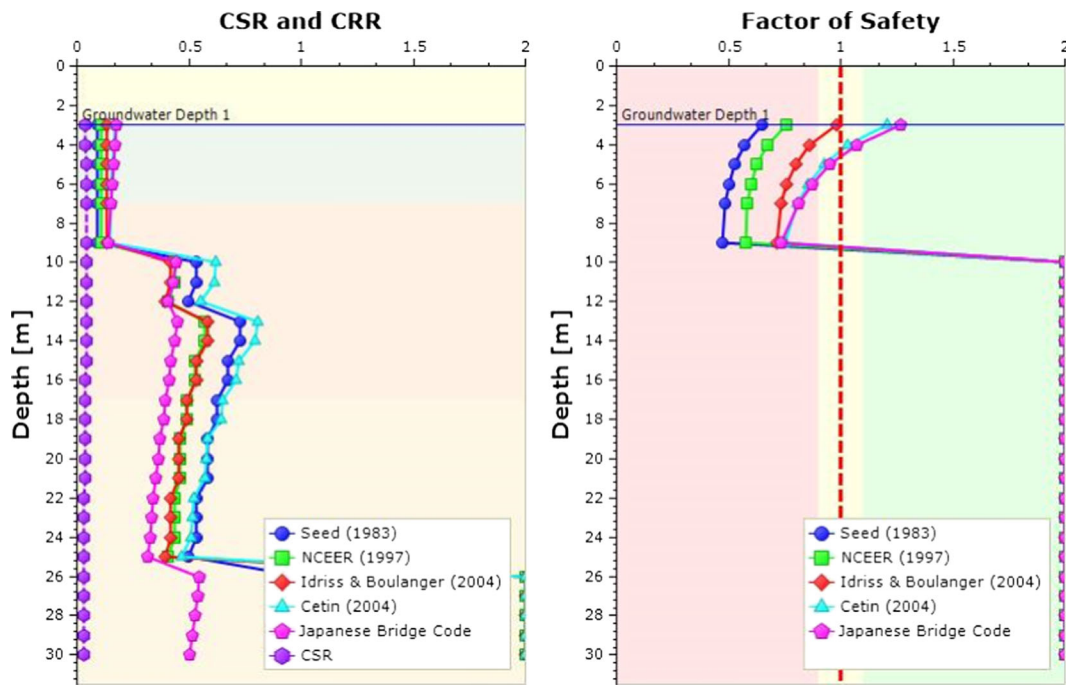


(c) SPT and stress reduction coefficient variation with depth for Zone 7, PGA=0.035g



(d) CSR, CRR, and Liquefaction potential variation with depth for Zone 7, PGA=0.035g

Fig. 10 (continued)



(e) CSR, CRR, and Liquefaction potential variation with depth for Zone 7, $PGA=0.06g$

Fig. 10 (continued)

layer. To verify the outcomes of the QUAKE/W models, liquefaction potential has also been assessed using a range of methodologies being used in the international seismic design industry (Seed et al. 2003; NCEER 1997; Idriss and Boulanger 2004; Cetin et al. 2004; and Al-Shayea 2005). In this paper, liquefaction analysis was carried out using the Settle3D software (Rocscience Inc.). The input consisted of seismic and geotechnical parameters for several subsurface strata layers. The seismic parameters used for the analysis are an acceleration range of 0.035 to 0.1 g and an earthquake of $M = 6.5$ generated from the Minagish fault (Kuwait) about 200 km towards the north of the study area. The geotechnical parameters used for the liquefaction analysis were the representative SPT N -values of soil layers in the study area. The software analyzes the liquefaction potential using magnitude scaling factor (MSF), fines content correction, and K_σ factor (an overburden correction factor used to adjust the cyclic stress ratio (CSR) or cyclic resistance ratio (CRR) to a common effective overburden stress) as per Idriss and Boulanger (2008), the stress reduction factor

(R_d) from Idriss (1999), relative density (D_r) estimation from SPT using the guidelines in Idriss and Boulanger (2003), and K_α factor (the static shear stress correction factor used to adjust CRR values for the effects of static shear stresses) as suggested by Idriss (2003). The liquefaction analysis results for the zones 1 and 7 using these empirical and analytical methodologies are shown in various parts of Fig. 10 (as per Boulanger (2003), Boulanger and Idriss (2004), Cetin and Bilge (2012), Cetin et al. (2009a, b)).

3 Results and discussions

Studies related to the geologic, geotechnical, hydrologic, and geotectonic morphologies of the area indicated the presence of wide variety of the subsurface strata at the study area. These strata generally consist of saline sabkha deposits overlain and underlain by the sandy layers of different origins. Sabkha soils are present, either as loose sand or soft clay layers, at the shallow depths, and



Fig. 11 Subsurface strata zoning map of the study area showing ten seismogenic zones

vary in thickness from 2.0 to 6.0 m. Sabkha, at most of the places, is underlain by the very dense sands and hard, heavily overconsolidated clays of Hadruk formation. Figure 7 reveals that the fines content for sandy sabkha layers ranges from 6 to 11%, while that for clayey sabkha ranges from 60 to 75%. Low fines content of the sandy sabkha layers makes them prone to liquefaction even at low PHA of 0.06 g, while clayey sabkha layers have resistance to liquefaction owing to the high fines of soft nature. These sabkha layers are covered with the backfilled and dune sand layers. High water tables have been encountered within 2.0 to 3.0 m from the ground surfaces.

Based on this variation of the subsurface conditions, the Jubail industrial city is divided into ten major seismic zones. These zones are listed below and are shown in Fig. 11, with a typical cross section drawn across the study area to the basement rock provided in Fig. 12.

1. Zone 1: PZ-1: soft clayey (sabkha) layer (2–3 m thick), fines content 60–75%, present at a depth of 2–3 m from surface
2. Zone 1A: PZ-1A: loose sandy (sabkha) layer (2–3 m thick), fines content 6–11%, present at a depth of 2–3 m from surface
3. Zone 2: PZ-2: no sabkha layer
4. Zone 3: PZ-3: same as PZ-1, but with no hard clay (Hadruk) layer within 30.0 m depth
5. Zone 3A: PZ-3A: same as PZ-1A, but with no hard clay (Hadruk) layer within 30.0 m depth
6. Zone 4: PZ-4: soft clayey (sabkha) layer (3 m thick), fines content 60–75%, present at a depth of 2–3 m, and no clay (Hadruk) layer within 30.0 m depth
7. Zone 5: PZ-5A: loose sandy (sabkha) layer (4 m thick), fines content 6–11%, present at a depth of 2–3 m

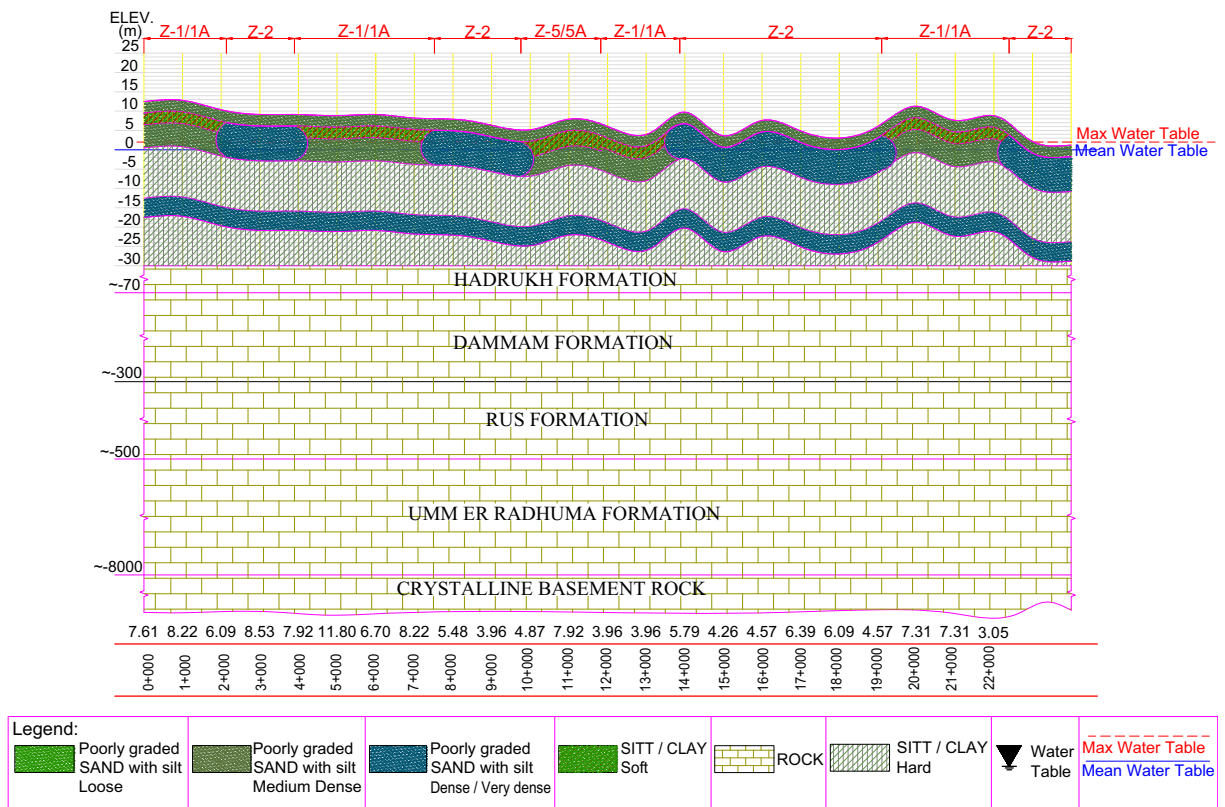


Fig. 12 A typical cross section (A-A') through the subsurface strata zoning map of the study area to the basement rock

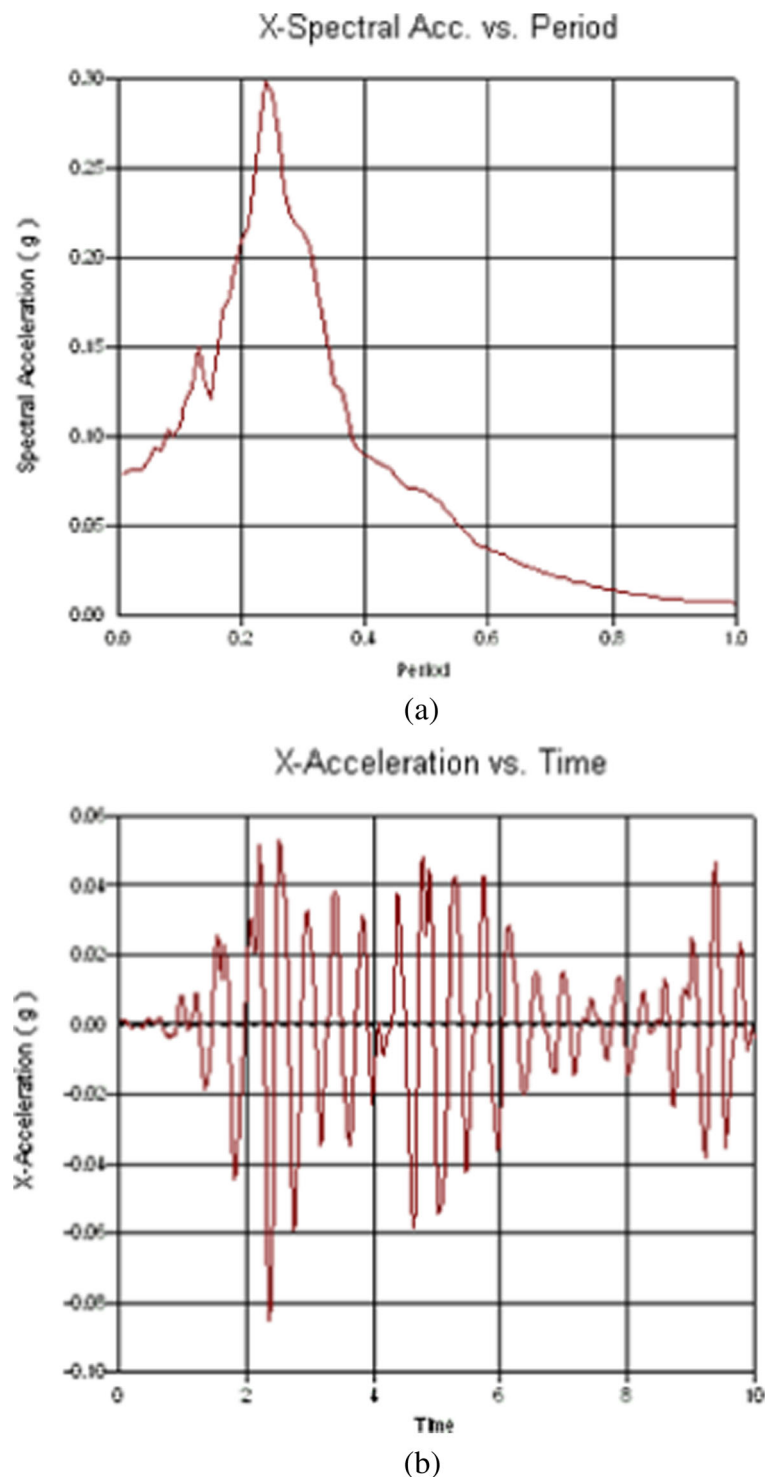
8. Zone 5A: PZ-5: soft clayey (sabkha) layer (4 m thick), fines content 60–75%, present at a depth of 2–3 m
9. Zone 6: PZ-6: same as PZ-5, but with no sabkha layer
10. Zone 7: PZ-7: loose sandy (sabkha) layer (6 m thick), fines content 6–11%, present at a depth of 2–3 m

Field and laboratory investigations, consisting of cross-hole seismic tests and cyclic triaxial tests, generated a range of dynamic parameters and their variations with the stress/strain for all the soil layers in each zone. For the detailed analysis purposes, the design profiles were also prepared for each of the ten subsurface zones. The design profiles for zone 1, zone 2, and zone 7 are shown in Fig. 7. These design profiles have been prepared based on the geotechnical and seismic parameters defined for each subsurface strata layer in Fig. 4. It can be noted

from Figs. 4 and 7 that low values of shear modulus (less than 1 MPa) were assigned to loose sand layers, while high values (1000 MPa) were assigned to the underlying sand layers. This sharp contrast between the moduli values of adjacent layers results in stress concentration and prolonged shaking of the loose layers under dynamic loading. A sharp increase in V_p values from the seismic test (Fig. 4) indicates the presence of water table at a depth of about 3.0 m.

The seismic response behavior of the software models, simulated under a synthetic earthquake, generated possible acceleration response and liquefaction potential scenarios, for various soil layers of each zone, under different PHA ranges. As a result of the analysis, probabilistic maximum considered ground motion is presented as the spectral response acceleration for any given period, T , with a 2% probability of being exceeded within 50 years. The result of the modeling is presented

Fig. 13 Dynamic analysis results for model 1 (Fig. 9) showing the response of surface node at PHA = 0.035 g. **a** Spectral acceleration against period. **b** Horizontal acceleration with time



as the horizontal nodal acceleration (S_a) and spectral acceleration at the surface for 5% damping ratio of the structure (Fig. 13). Site-specific

spectral acceleration responses for the surface layers of each zone are summarized in Table 2. The results in Fig. 13 indicate that the acceleration

was amplified from 0.035 g at the base to 0.085 g at the surface. Amplification factors up to 3.5 were observed in this study. Moreover, the values of the short period spectral acceleration at 0.2 s (S_s) and the long period spectral acceleration at 1 s (S_1) acquired in this study were found to be different than the ones suggested in some local codes. The S_s values evaluated from the model simulations are generally higher than the codes' specified value, while S_1 values are found to be lower than these suggested by the codes. This calls for the structures located in the study area to be re-evaluated.

The liquefaction potential for various seismic input scenarios is plotted on the map of the subsurface strata zonation of the area (Fig. 14), and is summarized in Table 2. Liquefaction potential of the study area is plotted for PHA of 0.035 and 0.10 g with the corresponding areas susceptible to liquefaction as hatched in Fig. 14. These results revealed that there is not a probability of liquefaction at the maximum PGA of 0.035 g. However, liquefaction could be anticipated at higher PGA values (≥ 0.055 g) for the various thicknesses of the loose sandy sabkha layers (Table 2). At PGA of 0.055 g, only subsurface strata with 6.0 m thick loose sand layers are expected to be liquefied, while at PGA of 0.1 g, all the zones

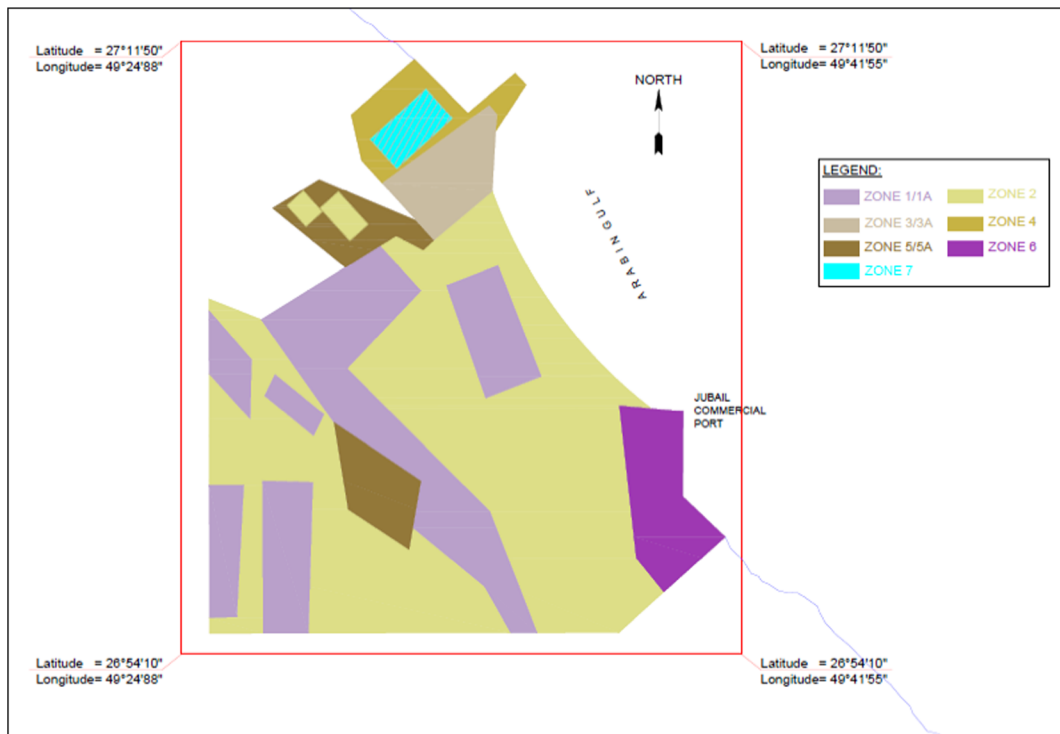
with loose sand layers are anticipated to be liquefied. Moreover, no liquefaction is expected even at higher PHA value of 0.35 g for the zones where sabkha layers are absent, and the subsurface layers consist only of sand layers.

Presence of high salt content in the sabkha soils may also affect the cyclic behavior of these soils. The effects of pore-water chemistry on the cyclic behavior of clayey sand were evaluated by Mesri and Olson (1970). They found a decrease in liquefaction potential with an increase in sodium chloride content. They attributed this behavior to the formation of agglomerates, reduction in plasticity, and hence the loss of cohesion at the particles' contacts. Similarly, Gratchev et al. (2004) evaluated the effects of pore-water chemistry on cyclic behavior of clayey sand. They used sodium chloride solution of different concentrations as the saturating fluid in clayey sand specimens. They found that sodium chloride causes a reduction in the plasticity of the clay fines and hence a corresponding reduction in the liquefaction resistance. In order to further confirm the effect of reduction in plasticity on liquefaction resistance, they also experimented the cyclic behavior of sand samples mixed with 15% of kaolin, illite, and bentonite

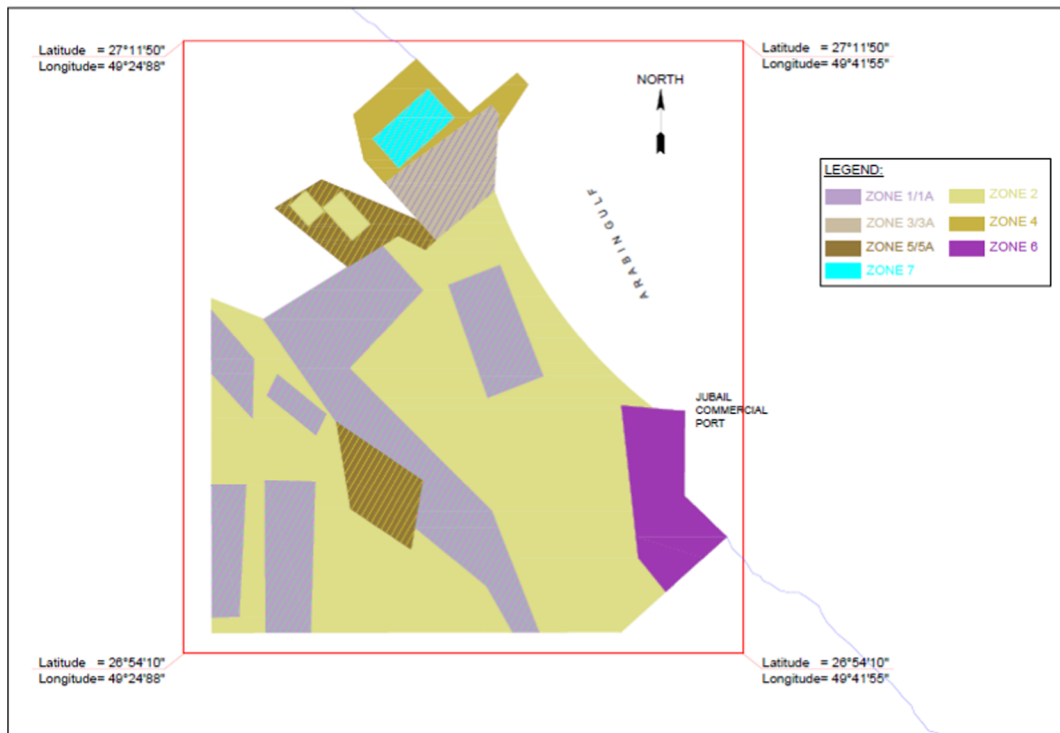
Table 2 Summary of dynamic simulation results using QUAKE/W

Case	Strata		Site class	a_{max} / g	Liquefaction potential	S_s	S_1	SAES-A-112	
	Loose / soft sabkha	Hard clay layer							
PZ-1	3.0 m Clayey sabkha	Present	D	0.035	No	0.11	0.02	S _s = 0.085	S ₁ = 0.031
PZ-1A	3.0 m Sandy sabkha	Present	D	0.035	No	0.1	0.025		
PZ-1A	3.0 m Sandy sabkha	Present	D	0.08	Yes	-	-		
PZ-2	No sabkha	Present	C	0.035	No	0.12	0.02		
PZ-3	3.0 m Clayey sabkha	Absent	D	0.035	No	0.14	0.02		
PZ-3A	3.0 m Sandy sabkha	Absent	D	0.035	No	0.11	0.025		
PZ-3A	3.0 m Sandy sabkha	Absent	D	0.10	Yes	-	-		
PZ-4	3.0 m Clayey sabkha	Absent	D	0.035	No	0.13	0.02		
PZ-5	4.0 m Sandy sabkha	Present	E	0.035	No	0.11	0.02		
PZ-5A	4.0 m Clayey sabkha	Present	E	0.035	No	0.12	0.025		
PZ-5A	4.0 m Clayey sabkha	Present	E	0.07	Yes	-	-		
PZ-6	No sabkha	Absent	C	0.035	No	0.12	0.02		
PZ-7	6.0 m Sandy sabkha	Absent	E	0.035	No	0.11	0.025		
PZ-7	6.0 m Sandy sabkha	Absent	E	0.055	Yes	-	-		

Red highlighted text indicates the occurrence of liquefaction



(a)



(b)

Fig. 14 Liquefaction potential map of various zones of the study area for **a** 0.055 g acceleration and **b** 0.1 g acceleration. Liquefaction prone zones are marked hatched

clay minerals. In these experiments, they discovered that kaolin, being the least plastic among the other two clay minerals, resulted in the least resistance to liquefaction. Based on these concepts, the presence of very high salt contents in the groundwater of the current study area seems to affect the fines present in the subsurface strata and may cause agglomeration and subsequent loss of cohesion/adhesion. Therefore, for this study, liquefaction resistance (or CRR) would have been decreased to a much lower degree in case of clayey sabkha, but would have been insignificant in case of sandy sabkha with little fines. Based on the same logic, the saline pore fluid would cause some reduction in liquefaction resistance (or CRR) in case of sand layers containing significant amount of clayey fines.

The liquefaction analysis performed using Settle3D software (Fig. 10) also reveals that no liquefaction is expected at the maximum anticipated PGA of 0.035 *g*, for both clayey and sandy sabkha layers. All the empirical and analytical methodologies employed in the software resulted in a factor of safety of more than one for the clayey sabkha soil layers under PGA of 0.035 *g*, which is in consistency with the results from the QUAKE/W modeling. Similarly, Fig. 10e also confirms the findings from the QUAKE/W modeling for the liquefaction potential of sandy sabkha layers at higher PGA of 0.06 *g*.

This validation of the liquefaction potential using both approaches confirms the reliability of the site-specific spectral acceleration response assessed through the QUAKE/W simulation analysis.

4 Conclusions and recommendations

This study indicates that the Jubail industrial area has a potential for seismic hazards. This is due to the presence of thick layers of loose sand at shallow depths and the close proximity to potential earthquake sources. Due to the presence of the petrochemical industrial setup in the area, the corresponding potential risk is also severe in nature.

Based on the heterogeneity of the type and thickness of the weak layers, the study area was divided into ten major seismic zones, with thicknesses of loose sandy sabkha layers ranging from

2 to 6 m. The sharp contrast in the static and dynamic parameters of the sabkha and the adjacent sand layers in these zones is expected to generate stress concentration, and prolonged shaking of the weak layers under the probable seismic loading. Although ten general zones were defined for the study area, the probability of several intermediate variations could also be possible. The corresponding risk assessment should be carried out for each project.

The results of this study indicate that there is not a significant probability of liquefaction of the loose sand layers at the maximum possible design PHA of 0.035 *g*. However, liquefaction is anticipated at higher PHA values (0.055, 0.07, 0.08, 0.10 *g*) for the subsurface profiles/zones with the corresponding thicknesses of 6, 4, 3, and 2 m thick for the loose sandy Sabkha soil layers. The results also indicate that no liquefaction potential exists for the subsurface strata having no sandy sabkha layers even at PHA values much higher than 0.35 *g*.

Site-specific spectral response assessment for the defined zones showed values for S_s and S_1 spectral accelerations, different than those suggested by local codes. The S_s values evaluated from the model were generally higher than those suggested by the code, while S_1 values were found to be lower than those suggested by the code. This indicates that the existing structures in the study area may need to be re-evaluated. Therefore, it is recommended that all the existing and future structures are to be analyzed and designed based on the probable seismic event using the spectral acceleration plots developed in this study for the corresponding zone (Table 2; Fig. 13).

Acknowledgements The authors highly acknowledge the support provided by King Fahd University of Petroleum & Minerals (KFUPM) and Riyadh Geotechnique & Foundations (RGF) during this research.

References

- Abdalla JA, Al-Homoud AS (2004a) Seismic hazard assessment of United Arab Emirates and its surroundings. *J Earthq Eng* 8(6):817–837
- Abdalla J.A. and Al-Homoud A.S. (2004b) “Earthquake hazard zonation of eastern Arabia”. *Proceedings of the 13th World*

- Conference on Earthquake Engineering, Vancouver, Canada, August 1–6, 2004, Paper No. 1008
- Al-Amoudi, O. S. B. (2008) “Testing and stabilization of saline sabkha soils: a review”, 6th International Conference on Case Studies in Geotechnical Engineering, Arlington, VA, 11–16 August 2008
- Al-Amri A.M. and Fnais M.S. (2009), “Seismic microzonation and site effect response of Dammam and Al-Khobar cities—Eastern Saudi Arabia”, Research proposal submitted to KACST
- Al-Amri A.M. and Fnais M.S. (2011). “Seismic microzonation and site effect response of Dammam and Al-Khobar cities”, KSU News <http://enews.ksu.edu.sa/2011/12/31/seismic-study/>.
- Al-Amri A, Rodgers A, Al-Khalifah T (2008) Improving the level of seismic hazard parameter in Saudi Arabia using earthquake location. *Arabian J Geosci* 1. doi:10.1007/s12517-008-0001-5, 1-15
- Al-Haddad M, Siddiqi GH, Al-Zaid R, Arafa A, Necioglu A, Turkelli N (1994) A basis for evaluation of seismic hazard and design criteria for Saudi Arabia. *Earthquake Spectra* 10(2):231–258
- Al-Sayari SS, Zofl JG (1978) Quaternary period in Saudi Arabia, 1. Springer, Wien
- Al-Shayea N (2005) “Evaluation of liquefaction potential at a petroleum site, Jeddah, Saudi Arabia”, Proceedings of the International Conference on Problematic Soils (GEOPROB 2005), Eastern Mediterranean University, Famagusta, N. Cyprus, 25–27 May 2005, Vol. 3, pp. 1039–1046
- Amir S, Wessel SK, Dam NS, Bo IL (2012) Manual for cyclic triaxial test. Aalborg University, Denmark
- ASTM D1586 (2011) Standard test method for standard penetration test (SPT) and split-barrel sampling of soils. American Society for Testing and Materials, West Conshohocken
- ASTM D3080/D3080M-11 (2011) “Standard test method for direct shear test of soils under consolidated drained conditions”, American Society for Testing and Materials
- ASTM D4015-15 (2015) “Standard test methods for modulus and damping of soils by fixed-base resonant column devices”, American Society for Testing and Materials
- ASTM D422-63 (2007), “Standard test method for particle-size analysis of soils”, American Society for Testing and Materials
- ASTM D4318-0e1 (2010) “Standard test methods for liquid limit, plastic limit, and plasticity index of soils”, American Society for Testing and Materials
- ASTM D4428/D4428M-07 (2007) “Standard test methods for crosshole seismic testing”, American Society for Testing and Materials
- ASTM D4767-11 (2011) “Standard test method for consolidated undrained triaxial compression test for cohesive soils”, American Society for Testing and Materials
- ASTM D5311-11 (2011) “Standard test method for load controlled cyclic triaxial strength of soil”, American Society for Testing and Materials
- Been K, Jefferies MG (1985) A state parameter for sands. *Geotechnique* 1985 35(3):123–132
- Benahmed, N., Canou, J. and Dupla, J.-C. (2015), “Liquefaction properties and initial structure of a loose sand”, 6th International Conference on Earthquake Geotechnical Engineering 1–4 November 2015 Christchurch, New Zealand
- Boore DM (2003) Simulation of ground motion using the stochastic method. *Pure Appl Geophys* 160:635–675
- Boulanger RW (2003) Relating $K\alpha$ to relative state parameter index. *J Geotech Geoenviron Eng ASCE* 129(8):770–773
- Boulanger RW, Idriss IM (2004). “State normalization of penetration resistances and the effect of overburden stress on liquefaction resistance.” Proc., 11th Intl. Conf. on Soil Dynamics and Earthquake Engineering, and 3rd Intl. Conf. on Earthquake Geotechnical Engineering, Doolin et al., eds, Stallion Press, Vol. 2, pp. 484–491
- Canou J (1989) Contribution à l'étude et à l'évaluation des propriétés de liquéfaction d'un sable. Ph.D. thesis. Ecole nationale des ponts et chaussées, Paris, 1989
- Cetin KO, Bilge HT (2012) Performance-based assessment of magnitude (duration) scaling factors. *J Geotech Geoenviron Eng* 138(3):324–334
- Cetin KO, Seed RB, Der Kiureghian A, Tokimatsu K, Harder LF Jr, Kayen RE, Moss RES (2004) SPT-based probabilistic and deterministic assessment of seismic soil liquefaction potential. *J Geotech Geoenviron Eng ASCE* 130(12):1314–1340
- Cetin KO, Bilge HT, Wu J, Kammerer AM, Seed RB (2009a) Probabilistic models for cyclic straining of saturated clean sands. *J Geotech Geoenviron Eng* 135(3):371–386
- Cetin KO, Bilge HT, Wu J, Kammerer AM, Seed RB (2009b) Probabilistic model for the assessment of cyclically induced reconsolidation (volumetric) settlements. *J Geotech Geoenviron Eng* 135(3):387–398
- Fnais MS (2011) “Ground-motion simulation for the eastern province of Saudi Arabia using a stochastic model”, Earthquake Resistant Engineering Structures VIII, 7–9 September 2011 Chianciano Terme, Italy
- Geo-Slope International Ltd (2003) www.geo-slope.com
- Gratchev IV, Sassa K, Fukuok H (2004) Cyclic behavior of clayey sands under different physico-chemical conditions. In: Lacerda, Ehrlich, Fontoura and Sayao (eds) Landslides: evaluation and stabilization, © 2004, Taylor and Francis Group, London p 701–704
- Idriss IM (1999) An update to the Seed-Idriss simplified procedure for evaluating liquefaction potential in Proceedings, TRB Workshop on New Approaches to Liquefaction, Publication No. FHWA-RD-99-165, Federal Highway Administration, January
- Idriss IM, Boulanger RW (2003) “Estimating $K\alpha$ for use in evaluating cyclic resistance of sloping ground”, Proc. 8th US Japan Workshop on Earthquake Resistant Design of Lifeline Facilities and Countermeasures against Liquefaction, Hamada, O'Rourke, and Bardet, eds., Report MCEER-03-0003, MCEER, SUNY Buffalo, N.Y., 449–468
- Idriss IM, Boulanger RW (2004) “Semi-empirical procedures for evaluating liquefaction potential during earthquakes”, Proc., 11th International conference on soil dynamics and earthquake engineering, and 3rd International conference on earthquake geotechnical engineering, vol. 1. Stallion Press; p. 32–56
- Idriss IM, Boulanger RW (2008) Soil liquefaction during earthquakes. Monograph MNO-12, earthquake. Engineering Research Institute, Oakland 261 pp
- James AN, Little AL (1994) Geotechnical aspects of sabkha at Jubail, Saudi Arabia. *Q J Eng Geol* 27(83–121):1994
- Joyner WB, Boore DM (1981) Peak horizontal acceleration and velocity from strong motion records including records from

- the 1979, Imperial valley, California earthquake. *Bull Seism Soc Am* 71:2011–2038
- Juneja A, Raghunandan ME (2010) “Effect of sample preparation on strength of sands”. Indian Geotechnical Conference—2010, GEOTrendz December 16–18, 2010 IGS Mumbai Chapter & IIT Bombay
- Kramer SL (1996) *Geotechnical earthquake engineering*. Prentice Hall, New Jersey
- Mesri G, Olson RE (1970) Shear strength of montmorillonite. *Geotechnique* 20(3):261–270
- Mitchell JK, Chatoion JM, Carpenter GC (1976) “The influences of sand fabric on liquefaction behaviors” Final report: S-76-5, US Army Waterway Station experimentation
- Mulilis JP, Seed HB, Chan JK, Mitchell JK, Arulanandan K (1977) Effects of sample preparation on sand liquefaction. *J Geotech Eng Div ASCE* 13(GT2):91–108
- NCEER, 1997 “Proceedings of the NCEER Workshop on Evaluation of Liquefaction Resistance of Soils”, Edited by Youd, T. L., Idriss, I. M., Technical Report No. NCEER-97-0022
- Pascucci V, Free MW, Lubkowski ZA (2008) “Seismic hazard and seismic design requirements for the Arabian Peninsula region”, The 14th World Conference on Earthquake Engineering October 12–17, 2008, Beijing
- Peiris N, Free M, Lubkowski Z, Hussein AT. (2006) “Seismic hazard and seismic design requirements for the Arabian Gulf region”, Proceedings of the 1st European Conference on Earthquake Engineering and Seismology, Geneva, Paper No. 1121
- RC Engineering Manual (2006) Chapter 9: design criteria: structural. Royal Commission for Jubail & Yanbu. Rocscience Inc. US <https://www.rocscience.com/>
- Sadek AW (2004) Seismic map for the state of Kuwait. *Emirates J Eng Res* 9(2):53–58
- Saudi Aramco Engineering Standard, SAES-A-112 (2013) “Meteorological and seismic design data”
- Saudi Building Code, SBC-303 (2007) Structural-soils and foundations. Saudi Building Code National Committee, Building Standards, Saudi Arabia
- Saudi Geological Survey (SGS) (2009). “Engineering Geology Map of Jubail Area”. http://www.sgs.org.sa/English/AppliedGeology/Pages/Engineering-Geology_en.aspx
- Seed RB, Cetin KO, Moss RES, Kammerer AM, Wu J, Pestana JM, Riemer MF, Sancio RB, Bray JD, Kayen RE, Faris A (2003) Recent advances in soil liquefaction engineering: a unified and consistent framework. 26th Annual ASCE Los Angeles Geotechnical Spring Seminar, Keynote Presentation, H.M.S. Queen Mary, Long Beach
- Tatsuoka F, Ochi K, Fujii S, Okamoto M (1986) Cyclic undrained triaxial and torsional shear strength of sands for different preparation methods. *Soils and Foundations* 1986 26(3):23–41
- USGS, 2013. <http://earthquake.usgs.gov/earthquakes/map>
- Vaid YP, Sivathyanan S, Stedman D (1999) Influence of specimen reconstituting method on the undrained response of sand. *Geotech Test J ASTM* 22(3):187–195
- Zlatovic S, Ishihara K (1997) Normalized behaviour of very loose non-plastic soils: effects of fabric. *Soils and Foundations* 1997 37(4):47–56